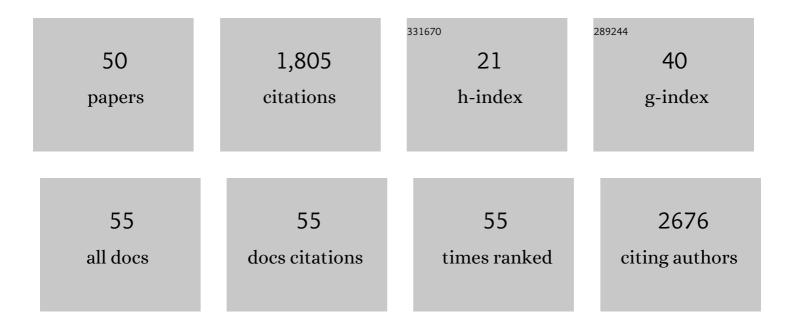
Simona Fermani

List of Publications by Year in descending order

Source: https://exaly.com/author-pdf/3859082/publications.pdf Version: 2024-02-01



#	Article	IF	CITATIONS
1	Redox regulation of the Calvin–Benson cycle: something old, something new. Frontiers in Plant Science, 2013, 4, 470.	3.6	355
2	Plant cytoplasmic GAPDH: redox post-translational modifications and moonlighting properties. Frontiers in Plant Science, 2013, 4, 450.	3.6	156
3	Gains and losses of coral skeletal porosity changes with ocean acidification acclimation. Nature Communications, 2015, 6, 7785.	12.8	106
4	Redox Homeostasis in Photosynthetic Organisms: Novel and Established Thiol-Based Molecular Mechanisms. Antioxidants and Redox Signaling, 2019, 31, 155-210.	5.4	95
5	Influence on the Formation of Aragonite or Vaterite by Otolith Macromolecules. European Journal of Inorganic Chemistry, 2005, 2005, 162-167.	2.0	86
6	Polymorphism and architectural crystal assembly of calcium carbonate in biologically inspired polymeric matrices â€. Dalton Transactions RSC, 2000, , 3983-3987.	2.3	75
7	Coral biomineralization: A focus on intra-skeletal organic matrix and calcification. Seminars in Cell and Developmental Biology, 2015, 46, 17-26.	5.0	71
8	Biomineralization control related to population density under ocean acidification. Nature Climate Change, 2014, 4, 593-597.	18.8	68
9	Conformational Selection and Folding-upon-binding of Intrinsically Disordered Protein CP12 Regulate Photosynthetic Enzymes Assembly. Journal of Biological Chemistry, 2012, 287, 21372-21383.	3.4	57
10	Calvin–Benson cycle regulation is getting complex. Trends in Plant Science, 2021, 26, 898-912.	8.8	57
11	Films of self-assembled purely helical type I collagen molecules. Journal of Materials Chemistry, 2004, 14, 2297.	6.7	44
12	High-Resolution Crystal Structure and Redox Properties of Chloroplastic Triosephosphate Isomerase from Chlamydomonas reinhardtii. Molecular Plant, 2014, 7, 101-120.	8.3	43
13	Coenzyme Site-directed Mutants of Photosynthetic A4-GAPDH Show Selectively Reduced NADPH-dependent Catalysis, Similar to Regulatory AB-GAPDH Inhibited by Oxidized Thioredoxin. Journal of Molecular Biology, 2004, 340, 1025-1037.	4.2	40
14	Glutathionylation primes soluble glyceraldehyde-3-phosphate dehydrogenase for late collapse into insoluble aggregates. Proceedings of the National Academy of Sciences of the United States of America, 2019, 116, 26057-26065.	7.1	39
15	Thioredoxin-dependent Redox Regulation of Chloroplastic Phosphoglycerate Kinase from Chlamydomonas reinhardtii. Journal of Biological Chemistry, 2014, 289, 30012-30024.	3.4	33
16	Customizing Properties of Î ² -Chitin in Squid Pen (Gladius) by Chemical Treatments. Marine Drugs, 2014, 12, 5979-5992.	4.6	31
17	Tuning Cysteine Reactivity and Sulfenic Acid Stability by Protein Microenvironment in Glyceraldehyde-3-Phosphate Dehydrogenases of <i>Arabidopsis thaliana</i> . Antioxidants and Redox Signaling, 2016, 24, 502-517.	5.4	31
18	β-Chitin samples with similar microfibril arrangement change mechanical properties varying the degree of acetylation. Carbohydrate Polymers, 2019, 207, 26-33.	10.2	26

Simona Fermani

#	Article	IF	CITATIONS
19	Crystallographic Control of the Hydrothermal Conversion of Calcitic Sea Urchin Spine (<i>Paracentrotus lividus</i>) into Apatite. Crystal Growth and Design, 2010, 10, 5227-5232.	3.0	25
20	Crystallographic Analysis of Metalâ€lon Binding to Human Ubiquitin. Chemistry - A European Journal, 2011, 17, 1569-1578.	3.3	25
21	<i>Arabidopsis</i> and <i>Chlamydomonas</i> phosphoribulokinase crystal structures complete the redox structural proteome of the Calvin–Benson cycle. Proceedings of the National Academy of Sciences of the United States of America, 2019, 116, 8048-8053.	7.1	25
22	Structural probing of Zn(ii), Cd(ii) and Hg(ii) binding to human ubiquitin. Chemical Communications, 2008, , 5960.	4.1	24
23	Structural and Biochemical Insights into the Reactivity of Thioredoxin h1 from Chlamydomonas reinhardtii. Antioxidants, 2019, 8, 10.	5.1	24
24	Shell properties of commercial clam Chamelea gallina are influenced by temperature and solar radiation along a wide latitudinal gradient. Scientific Reports, 2016, 6, 36420.	3.3	22
25	The 1.4Ã structure of dianthin 30 indicates a role of surface potential at the active site of type 1 ribosome inactivating proteins. Journal of Structural Biology, 2005, 149, 204-212.	2.8	21
26	Structure/function studies on two type 1 ribosome inactivating proteins: Bouganin and lychnin. Journal of Structural Biology, 2009, 168, 278-287.	2.8	19
27	Structure and Function of Stony Coral Intraskeletal Polysaccharides. ACS Omega, 2018, 3, 2895-2901.	3.5	19
28	Acidic Monosaccharides become Incorporated into Calcite Single Crystals**. Chemistry - A European Journal, 2020, 26, 16860-16868.	3.3	17
29	Crystal Structure of Chloroplastic Thioredoxin f2 from Chlamydomonas reinhardtii Reveals Distinct Surface Properties. Antioxidants, 2018, 7, 171.	5.1	16
30	Wavy graphene sheets from electrochemical sewing of corannulene. Chemical Science, 2021, 12, 8048-8057.	7.4	15
31	High Amino Acid Lattice Loading at Nonambient Conditions Causes Changes in Structure and Expansion Coefficient of Calcite. Chemistry of Materials, 2020, 32, 4205-4212.	6.7	14
32	Unravelling the shape and structural assembly of the photosynthetic GAPDH–CP12–PRK complex from <i>Arabidopsis thaliana</i> by small-angle X-ray scattering analysis. Acta Crystallographica Section D: Biological Crystallography, 2015, 71, 2372-2385.	2.5	13
33	Influence of proteins on mechanical properties of a natural chitin-protein composite. Acta Biomaterialia, 2021, 120, 81-90.	8.3	13
34	Structural and functional insights into nitrosoglutathione reductase from Chlamydomonas reinhardtii. Redox Biology, 2021, 38, 101806.	9.0	12
35	Structure of photosynthetic glyceraldehyde-3-phosphate dehydrogenase (isoformA4) fromArabidopsis thalianain complex with NAD. Acta Crystallographica Section F: Structural Biology Communications, 2010, 66, 621-626.	0.7	11
36	Structural basis for the magnesium-dependent activation of transketolase from Chlamydomonas reinhardtii. Biochimica Et Biophysica Acta - General Subjects, 2017, 1861, 2132-2145.	2.4	11

SIMONA FERMANI

#	Article	IF	CITATIONS
37	Coral micro- and macro-morphological skeletal properties in response to life-long acclimatization at CO2 vents in Papua New Guinea. Scientific Reports, 2021, 11, 19927.	3.3	10
38	Synthesis and Adsorbing Properties of Tabular {001} Calcite Crystals. Crystals, 2019, 9, 16.	2.2	9
39	Ecological relevance of skeletal fatty acid concentration and composition in Mediterranean scleractinian corals. Scientific Reports, 2017, 7, 1929.	3.3	8
40	Crystallization and preliminary X-ray diffraction analysis of two ribosome-inactivating proteins: lychnin and dianthin 30. Acta Crystallographica Section D: Biological Crystallography, 2003, 59, 1227-1229.	2.5	7
41	In Vitro Coral Biomineralization under Relevant Aragonite Supersaturation Conditions. Chemistry - A European Journal, 2019, 25, 10616-10624.	3.3	6
42	Structural snapshots of nitrosoglutathione binding and reactivity underlying S-nitrosylation of photosynthetic GAPDH. Redox Biology, 2022, 54, 102387.	9.0	6
43	Conformational Selection of Ubiquitin Quaternary Structures Driven by Zinc Ions. Chemistry - A European Journal, 2013, 19, 15480-15484.	3.3	5
44	Hierarchical chitinous matrices byssus-inspired with mechanical properties tunable by Fe(III) and oxidation. Carbohydrate Polymers, 2021, 251, 116984.	10.2	5
45	Exploring Coral Calcification by Calcium Carbonate Overgrowth Experiments. Crystal Growth and Design, 2022, 22, 5045-5053.	3.0	4
46	Climate variation during the Holocene influenced the skeletal properties of Chamelea gallina shells in the North Adriatic Sea (Italy). PLoS ONE, 2021, 16, e0247590.	2.5	2
47	Multiscale analysis on otolith structural features reveals differences in ontogenesis and sex in <i>Merluccius merluccius</i> in the western Adriatic Sea. Royal Society Open Science, 2022, 9, .	2.4	2
48	Aggregation Pathways of Native‣ike Ubiquitin Promoted by Singleâ€Point Mutation, Metal Ion Concentration, and Dielectric Constant of the Medium. Chemistry - A European Journal, 2018, 24, 4140-4148.	3.3	1
49	The skeleton of Balanophyllia coral species suggests adaptive traits linked to the onset of mixotrophy. Science of the Total Environment, 2021, 795, 148778.	8.0	1
50	Cholesterol derivatives make large part of the lipids from epidermal molts of the desert-adapted Gila monster lizard (Heloderma suspectum). Scientific Reports, 2020, 10, 17197.	3.3	0